JGR Atmospheres

RESEARCH ARTICLE
10.1029/2019JD030962

Deep Convective Evolution From Shallow Clouds Over the Amazon and Congo Rainforests

Sudip Chakraborty[1], Jonathan H. Jiang[1], Hui Su[1], and Rong Fu[2]

[1]Jet Propulsion Laboratory, California Institute of Technology, Pasadena, CA, USA, [2]Department of Atmospheric and Oceanic Sciences, University of California, Los Angeles, CA, USA

Key Points:
- The afternoon shallow clouds over the Congo region suppress evening deep convection and weaken the evening storm top height and rain rate
- Shallow clouds over the Amazon region promote growth of the evening deep convective cloud
- The relationship between afternoon shallow clouds and evening deep convection systems over the Congo and Amazon regions is different

Correspondence to:
S. Chakraborty,
sudip.chakraborty@jpl.nasa.gov

Citation:
Chakraborty, S., Jiang, J. H., Su, H., & Fu, R. (2020). Deep convective evolution from shallow clouds over the Amazon and Congo rainforests. *Journal of Geophysical Research: Atmospheres*, *125*, e2019JD030962. https://doi.org/10.1029/2019JD030962

Received 11 MAY 2019
Accepted 16 DEC 2019
Accepted article online 19 DEC 2019

Abstract Using satellite measurements from A-Train constellation and Global Precipitation Measurement mission, we investigate the relationships between the afternoon time shallow convective top height ($CTH_{afternoon}$) and the evening time deep convective storm top height ($CTH_{evening}$) and rain rate ($RR_{evening}$) over the Amazon and Congo regions. We use CloudSat cloud type stratus and stratocumulus as the shallow afternoon clouds. Our results indicate that the afternoon shallow clouds over the Congo region are associated with suppressed and weakened evening time deep convection, whereas shallow clouds over the Amazon region are associated with the growth of the evening time deep convection. Over the Congo region, we find that as $CTH_{afternoon}$ increases, shallow convective rain rate in the afternoon ($RR_{afternoon}$) increases. As a result, the evening time convective available potential energy (CAPE) as well as free tropospheric humidity ($RH_{700\text{-}300}$) decrease. Consequently, condensation occurring inside deep convection reduces and $CTH_{evening}$ as well as $RR_{evening}$ decrease over there. Over the Amazon region, however, $RR_{afternoon}$ does not vary significantly with $CTH_{afternoon}$. As $CTH_{afternoon}$ increases, CAPE, $RH_{700\text{-}300}$, and condensation occurring inside deep convection increase in the evening. As a result, deep convective $CTH_{evening}$ and $RR_{evening}$ increase with $CTH_{afternoon}$ over the Amazon basin. These dissimilarities in the ambient condition drive the shallow to deep convective evolution differently over these two rainforests. On the other hand, shallow clouds that remain shallow in the evening are associated with less CAPE and $RH_{700\text{-}300}$, $RR_{afternoon}$, and $RR_{evening}$. Although CAPE and $RH_{700\text{-}300}$ promote deep convection to a height cloud top height, high vertical wind shear inhibits deep convection.

1. Introduction

Tropical rainforests harbor the largest biodiversity over the land and play crucial roles in global carbon storage, hydrological cycle, carbon cycle, and global climate change (Laurance et al., 1999; Salati & Vose, 1984). Rainforests over the Amazon and Congo have been hit by a series of recent and past droughts, and a lack of rainfall along with a continued deforestation (Tyukavina et al., 2018) due to agricultural demand has posed a threat to the future existence of the rainforests (Cox et al., 2004; Phillips et al., 2009). It is expected that the African drylands might intrude southward under a warming climate (Feng & Fu, 2013). The deforestation rate is declining over the Amazon region; however, drought-related forest fires have gone up and are counteracting the effects of such declines (Aragao et al., 2018). A recent study by Zhou et al. (2014) shows that the greenness over the Congo rainforest is declining in recent years as the rainfall has declined at a rate of 0.32 ± 0.10 mm/day per decade over last 50 years. Such rate is even stronger and shaper in the northern tropical Africa (Malhi & Wright, 2004). Thus, it has been suggested in the literature that there should be a priority and need to understand the rainfall variability over these two regions, especially over the Congo rainforest owing to its long drying trend and global warming (Malhi & Wright, 2004; Zhou et al., 2014). Thus, understanding and predicting rainfall variability over these two rainforests are tremendously important.

On the other hand, variability in rainfall, which is the primary factor for the sustainability of these rainforests, is poorly represented in climate models. Climate models often fail to predict rainfall accurately over both rainforests and also exhibit large uncertainties in rainfall projections (Vera et al., 2006). Poor parameterization and difficulties in simulating shallow to deep convection evolution over the Amazon (Li et al., 2006; Vera et al., 2006) and inadequate understanding of the observed rainfall variability as well as its relationships with African easterly jets and local meteorology (Washington et al., 2013; Whittleston et al., 2017) contribute to large uncertainties in rainfall simulations and projections in climate models. For example, it is known that African jets play an important role in regulating rainfall variabilities (Nicholson, 2017;

Nicholson & Dezfuli, 2013); however, a recent study by Whittleston et al. (2017) shows that many CMIP5 models fail to capture the couplings between the rainfall and jets over Africa.

Deep convection is the primary source of tropical precipitation (Houze, 2004); therefore, identifying the influence of afternoon shallow clouds on evening deep convective clouds is important to understand the rainfall variability and wet season onset over Amazon and Congo rainforests (Del Genio & Wu, 2010; Jensen & Del Genio, 2006). In a recent study, Raghavendra et al. (2018) identifies that even if the Congo rainforest rainfall is declining, the intensity and the extent of the storms are increasing over there. These results propel us to understand the shallow to deep convective evolution mechanism over the rainforests, especially over the Congo. Many studies have attempted to understand the shallow to deep convection evolution over the Amazon region (Chakraborty, Schiro, et al., 2018; Zhuang et al., 2017) where shallow clouds in the transition season have been observed to gradually moisten up and destabilize the free troposphere, thus making it suitable for deep convective growth (Wright et al., 2017). However, it is not clear whether such processes also occur over the Congo region, the world's second largest rainforest. The rainfall variability over the Congo region is complex, less understood or analyzed compared to that over the Amazon rainforest. A lack of understanding of such processes from observations adversely impacts climate model improvements.

Moreover, atmospheric dynamics and meteorological conditions of these two regions are different. Zonal easterly jets dominate the African continent and are responsible for many equatorward cyclogeneses over the region (Nicholson, 2017; Nicholson & Dezfuli, 2013). Moisture source over the Congo region is below 850 hPa from the Atlantic Ocean (Dezfuli & Nicholson, 2013; Neupane, 2016) Above 850 hPa, there tends to be an intrusion of dry air from the Saharan region (Dezfuli & Nicholson, 2013). On the other hand, such easterly jets are absent over the Amazon region and moist air is advected from the Atlantic Ocean by northeasterly trade wind or the lower-level jets (Fu et al., 1999, 2001; Molion, 1975) during the wet season. Vertically integrated moisture convergence is important to understand rainforest rainfall mechanism. A recent study found out that zonal (meridional) wind convergence is important over the Amazon (Congo) rainforest (https://ams.confex.com/ams/98Annual/webprogram/Paper329215.html). Thus, the shallow to deep convective evolution over these two regions might be different. This study aims to investigate and compare the shallow to deep convective evolution over the two regions. To our knowledge, such analyses have not been conducted before, especially over the Congo region.

Understanding such processes using the satellite data requires a large number of samples of the afternoon shallow convection and the evening deep convection over the same location. By collocating measurements from A-Train satellites in the afternoon and the Global Precipitation Measurement (GPM) mission in the evening, we investigate how the afternoon shallow convective rain rate ($RR_{afternoon}$) and cloud top height ($CTH_{afternoon}$) associated with shallow clouds influence the evening time condensation, rain rate ($RR_{evening}$), and storm top height ($CTH_{evening}$) of deep convection over Congo and Amazon. Section 2 discusses the data and methodology of the study. Results are presented in section 3, and conclusions are given in section 4.

2. Data and Methods

2.1. Data Sets

We use A-Train measurements and Integrated Multisatellite Retrievals for GPM (IMERG) data sets to obtain information about $CTH_{afternoon}$ and $RR_{afternoon}$ around 1:30 p.m. local time. Information about deep convection in the evening, such as latent heat (LH), $RR_{evening}$, and $CTH_{evening}$ are gathered from GPM data sets. Information about various meteorological conditions are obtained from the Modern Era Retrospective-Analysis for Research and Applications (MERRA2) data sets.

2.1.1. TERRA MODIS

Moderate Resolution Imaging Spectroradiometer (MODIS) onboard TERRA satellite with a 2,330-km-wide swath has 36 discrete spectral bands. We use 10-km resolution aerosol optical depth (AOD) data (MOD04) for this analysis. Details of these data sets are available online (https://modis.gsfc.nasa.gov/data/dataprod/mod04.php). AOD data sets from TERRA MODIS have been validated over land and ocean (Chu et al., 2002; Remer et al., 2002). We use TERRA AOD measured at 10 a.m. local solar time in our analysis because Aqua MODIS AOD is compromised by the afternoon shallow cloud appearance over the region. TERRA, on

the other hand, flies in the morning and is more likely to detect aerosols when clouds are absent in the morning but appear in the afternoon.

2.1.2. CloudSat

CloudSat is a 94-GHz cloud profiling radar with a wavelength of 3 mm, which flies in a Sun-synchronous orbit. It measures the power backscattered from the clouds and provides cloud profiles at a vertical resolution of 240 m and horizontal resolution of 1.4 (across track) × 1.7 km (along track). We have used Cloudsat data sets for the identification of shallow clouds in the afternoon and 2B-CloudClass data for the information of cloud top height of shallow clouds. Only day time CloudSat data set is used for the period of March 2014 to December 2017 (whenever available). Details of the CloudSat data sets are available online (http://www.cloudsat.cira.colostate.edu/data-products).

2.1.3. CALIPSO

Like CloudSat, Cloud-Aerosol Lidar and Infrared Pathfinder Satellite Observations (CALIPSO) is another satellite in the A-Train constellation. Flying right after CloudSat, it is designed to observe the aerosols along an almost similar track to CloudSat. We use Level 2 Version 3.01 vertical feature mask (VFM) data sets. It has a resolution of 0.33–5 km in the horizontal and 30–180 m in the vertical. It operates at two wavelengths of 532 and 1,064 nm. To avoid the misclassifications between the clouds and aerosols, we use the VFM data based on five different parameters [*J J* Liu et al., 2014; *Z Y* Liu et al., 2009]. It provides a cloud or aerosol discrimination score between −100 to 100. We use data with an absolute CAD score greater than 70 to avoid the ambiguities that can arise due to the presence of clouds. Use of CAD score reduces the uncertainty in the misclassification to 2.1%. CALIPSO data have previously been used extensively for aerosol studies (Chakraborty et al., 2015; Redemann et al., 2012). CALIPSO provides aerosol information as pixels in which aerosols are detected in the VFM data, unlike MODIS, which provides AOD.

2.1.4. AIRS

To gather information about the moisture associated with shallow and deep clouds, we use Atmospheric Infrared Sounder (AIRS) water vapor mixing ratio (MR) and columnar water vapor (CWV) data sets for this analysis. Level 2 water vapor MR is available from the surface to the upper troposphere at a vertical resolution between 50 and 100 hPa at 20 different levels since 2002. AIRS data sets are available online (https://airs.jpl.nasa.gov/data/get_data). AIRS measures radiances within the infrared spectrum from 3.7 to 5.4 μm (Jones & Stensrud, 2012) and has a horizontal resolution of 13.5 and 45 km. It provides data two times a day and is a member of the A-Train constellation (https://docserver.gesdisc.eosdis.nasa.gov/repository/Mission/AIRS/3.3_ScienceDataProductDocumentation/3.3.4_ProductGenerationAlgorithms/V6_L2_Product_User_Guide.pdf). Thus, it provides nearly simultaneous information about the water vapor associated with the clouds observed by CloudSat and the aerosols observed by CALIPSO. It has been used for many scientific studies and has been extensively evaluated against independent observations (Hagan et al., 2004; Jones & Stensrud, 2012). We use MR data provided at 20 different levels and CWV form AIRS data for this analysis.

2.1.5. GPM

The evening rain rate ($RR_{evening}$), cloud top height ($CTH_{evening}$), and LH profiles of deep convection clouds are analyzed from the GPM data sets. GPM, built on Tropical Rainfall Measurement Mission's legacy, provides global rainfall and snow measurements worldwide every 3 hr (https://www.nasa.gov/20mission_pages/GPM/overview/index.html). It flies at an altitude of 407 km with a non-Sun-synchronous orbit and measures the Earth's rainfall within a much wider (65°N to 65°S) latitude band than Tropical Rainfall Measurement Mission. It has a dual frequency radar that scans across as 125 km (35.5-GHz Ka-band) and 254 km (13.6-GHz Ku band) with a resolution of 5 km. It also has a Microwave Imager (GMI) that scans at 13 channels with variables frequencies that range from 10.65 to 183.3 GHz. Thus, GPM can detect rain droplets of various sizes, storm top height, and cloud particles inside a cloud owing to the radar's wide scanning frequencies.

We have used 2HSLH or the spectral latent heating data product to obtain LH associated with the deep convection in the evening. The 2HSLH is an instantaneous Level 2 Version 6 data with 5 km of spatial resolution. The data are provided in 80 vertical levels.

Along with the satellite data sets in the evening time, we also use 30-min gridded (0.1° × 0.1°) IMERG (Sungmin et al., 2017) to estimate $RR_{afternoon}$ associated with the shallow clouds in the afternoon between 1,330 and 1,430 pm observed by CloudSat. Details about the IMERG data are available at https://pps.gsfc.

nasa.gov/Documents/IMERG_ATBD_V4.pdf (Huffman et al., 2014). Satellite rainfall products, when compared with GPCP rain gauge measurements well reproduce the seasonal cycle and the latitudinal gradients of rainfall (Nicholson et al., 2019).

2.1.6. MERRA2

We have used the MERRA data sets for the calculation of convective available potential energy (CAPE) and free tropospheric relative humidity ($RH_{700\text{-}300}$). We have used 3-hourly, instantaneous, pressure level, assimilated meteorological fields data sets (inst3_3d_asm) to evaluate CAPE from the temperature and specific humidity data sets. RH in the free troposphere is calculated as the mean of RH between 700 and 300 hPa. These data sets are provided at 0.5° × 0.625° resolutions in the latitudinal and longitudinal direction every 3 hr and are available to the public for downloading (https://gmao.gsfc.nasa.gov/reanalysis/MERRA-2/data_access/). For Congo (Amazon), we use data sets at 1500 (2100) UTC to estimate CAPE and RH. We also compute VWS from MERRA2 data. VWS was computed as a difference in mean wind speed between the low level (850–900 hPa) and upper level (200–250 hPa) (Chakraborty, Fu, et al., 2018; Petersen et al., 2006). We choose MERRA reanalysis since the analyses have been performed near the A-Train constellation track. Although large spread is found in the performance among different reanalysis products over the Congo basin (Cook & Vizy, 2016), Hua et al. (2019) found out that MERRA2, when compared with all other major reanalysis data sets, is the best reanalysis product that reproduces the mean climatology and interannual variability over the Congo basin. They have also found out that MERRA2 data also have the smallest biases and root-mean-square error in describing the wind fields in the lower to middle-troposphere, thus making it suitable for our meteorological analysis.

2.2. Methods

We use CloudSat data sets to identify shallow convective clouds and their cloud top height in afternoon around 1:30 p.m. local time. GPM IMERG data sets have been used to measure shallow convective rain rate in the afternoon (between 1:30 p.m. and 2:30 p.m.). GPM 2BCMB data sets have been used to calculate deep convective rain rate and cloud top height about 2–4 hr after the A-Train overpasses. Using information from various satellite data sets enables us to identify the relationship between afternoon shallow clouds and evening deep convection systems over these two regions. We obtain 888 and 918 cases within the period from March 2014 to December 2017 over the Amazon and Congo regions, respectively.

We use CloudSat CloudClass data sets to identify shallow clouds in the afternoon during the A-Train overpass around 1:30 p.m. local time. CloudClass data sets identify eight different cloud types, such as cirrus, altostratus, altocumulus, status, stratocumulus, cumulus, nimbostratus, and deep convection. After identifying shallow clouds (stratocumulus and stratus) over the domain of interest, we estimate the cloud top height of shallow clouds from the CloudSat data. We only use stratus and stratocumulus cloud types since CloudSat cloud classification identifies those as shallow clouds (Sassen & Wang, 2008). We exclude cumulus cloud type from our analysis since it is defined as a low as well as moderately thick clouds (Wang & Sassen, 2001). To compute the $CTH_{afternoon}$, we first identify the shallow (stratus and stratocumulus) along the CloudSat track. We perform such identifications by dividing the region in 2° × 2° sized grid boxes. After we identify the shallow clouds in a box, we check the maximum height of the cloud from CloudClass data and denote it as $CTH_{afternoon}$. In order to minimize the impact of the assumption that the evening time clouds have spawned from the afternoon clouds, we have only used those grids where we did not observe any deep cloud in the afternoon. This method allows us to remove those shallow clouds that were already in the vicinity of any other deep cloud that might propagate to the shallow cloud locations. Grids with shallow clouds only in the afternoon are chosen for this analysis. We use the information about the location of shallow clouds from the CloudSat data sets to obtain AOD from TERRA MODIS, water vapor from AIRS, and aerosol vertical profiles from CALIPSO associated with the clouds. We estimate AOD surrounding shallow clouds within a radial distance of ±2° from the location of shallow clouds. This is to avoid erroneous detection of aerosols that may occur due to relative humidity bias (Remer et al., 2005; Tackett & Di Girolamo, 2009) and 3-D radiative transfer (Varnai & Marshak, 2009) when aerosols are present near the clouds. Previous studies show that this approximation is reasonable for avoiding influences from other clouds, and misclassifications as well as erroneous detection of aerosols for any level of AOD that surrounds the clouds (Chakraborty et al., 2015, 2016; Chakraborty, Fu, et al., 2018). AIRS water vapor data sets are used to calculate CWV and MR profiles at different pressure levels surrounding shallow clouds. We derive the

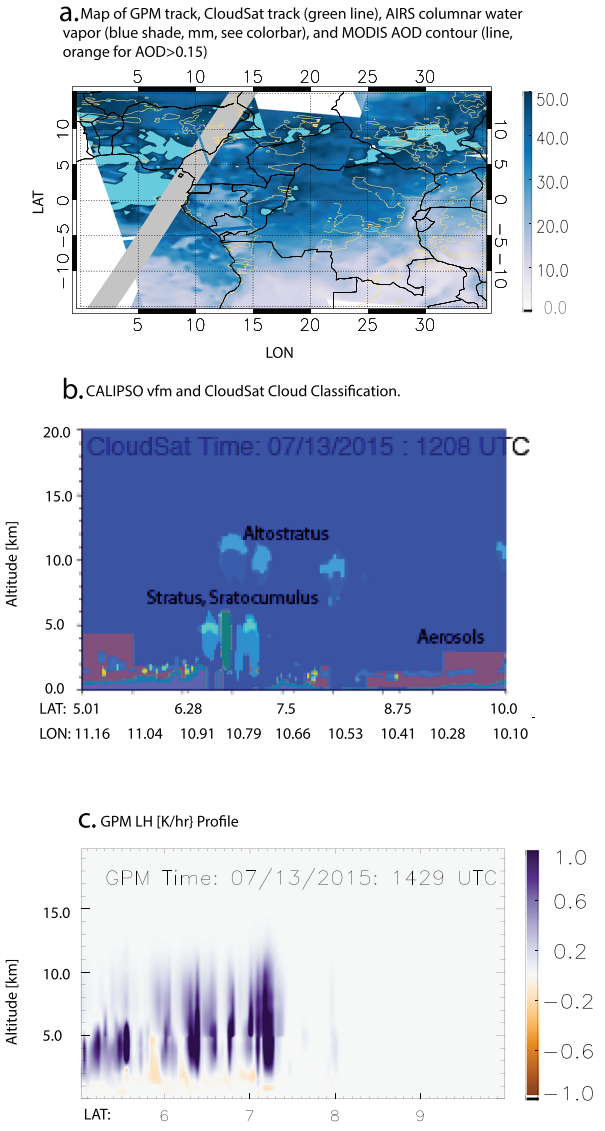

Figure 1. Collocation of GPM, CloudSat, CALIPSO, AIRS, and Terra MODIS aerosols over the Congo region on 13 July 2015. Panel (a) shows the AIRS water vapor (shaded contour), MODIS (orange lines) AOD, CloudSat track (green line), and GPM track. Panel (b) shows the CloudSat stratus and altocumulus clouds and CALIPSO detected VFM aerosols pixels. Panel (c) shows the GPM LH profiles at 1429 UTC.

number of aerosol pixels from CALIPSO data sets at each level surrounding shallow clouds at a radial distance of ±2° to avoid any misclassifications in cloud-aerosol discrimination near the cloud periphery.

GPM 2B_CMB data sets provide information about the evening deep convective clouds over the same location. To search cases where an afternoon shallow cloud develops into a deep convective cloud in the evening, we use $CTH_{afternoon}$ from CloudSat and the evening cloud top height from GPM ($CTH_{evening}$). We carry out searches for such events by dividing the domain into many 2 × 2° grids in the latitudinal and longitudinal directions. Once an afternoon shallow cloud is detected, we check if there is any deep convection developed in the evening time in the same grid and if so, we record their cloud top heights ($CTH_{afternoon}$ and $CTH_{evening}$). We use $RR_{evening}$ and $CTH_{evening}$ from GPM 2B_CMB data sets. If the $CTH_{evening}$ is greater than $CTH_{afternoon}$ and reaches above 8 km, then we calculate the shallow convective RR from the IMERG data at a radial distance of ±0.1° and ±0.2° from the center of shallow clouds (detected by CloudSat). We compute the evening time RR, LH, and $CTH_{evening}$ from the GPM data. We estimate the meteorological conditions, such as ambient relative humidity at the lower troposphere (RH_{850}) and in the free troposphere ($RH_{700\text{-}300}$), CAPE, in between the timing of the shallow and deep convection from MERRA2 (Chakraborty et al., 2016; Gelaro et al., 2017; Rienecker et al., 2011). We also compute AIRS water vapor to obtain meteorological information associated with shallow clouds. We use AOD from TERRA since it flies in the morning and is more likely to detect aerosols when clouds are absent in the morning but appear in the afternoon. Figure 1 shows an example of such collocations and the evolution from a shallow cloud in the afternoon to a deep cloud in the evening.

2.3. A Typical Case of Shallow to Deep Convection Evolution

Figure 1 shows the afternoon shallow clouds detected by the A-train satellites and the evening time deep convection detected by a GPM overpass over the same location. The bottom Figure 1a shows the CloudSat track (green line) over Cameroon and Nigeria at 12:08 UTC on 13 July 2015. The GPM track over that region passes at 14:29 UTC on the same day. Blue shades show the AIRS CWV over the region and the orange line contours show the AOD greater than 0.15 from TERRA MODIS. Figure 1b shows the CloudSat and CALIPSO profiles along the green track in Figure 1a. CloudSat detects stratus and stratocumulus clouds between 6.26° and 7.5° latitude. CALIPSO detects aerosol pixels (orange contours) elevated up to 4 km near the stratus and stratocumulus clouds. The evening time profile at the same location is shown in Figure 1c. Figure 1c shows GPM LH profiles over the same location up to an altitude of 12 km. LH profiles show the mean LH across the track and indicate that strong condensation occurs since the values are positive (up to ~2 K/hr). This figure illustrates an example of shallow clouds and associated AOD, CWV, aerosol pixels derived from the A-Train satellites in the afternoon and evening time deep clouds and related information, such as LH, $RR_{evening}$, and $CTH_{evening}$ derived from GPM over the same region. We have carried out analysis from March 2014 to December 2017 over the Amazon [5°N, 80°W, 15°S, 40°W] and Congo [10°N, 0°, 10°S, 32°E].

Our goal is to investigate how the afternoon $RR_{afternoon}$, $CTH_{afternoon}$, ambient water vapor, and AOD from TERRA MODIS affect the evening time deep convective properties and to find out how afternoon shallow clouds affect shallow to deep convection evolution.

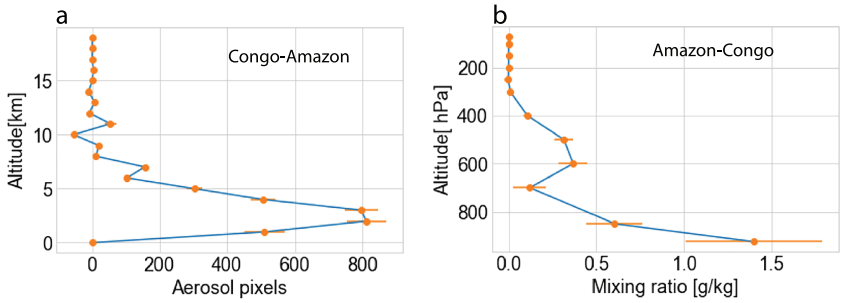

Figure 2. Differences in mean (a) number of aerosol pixels from CALIPSO (Congo-Amazon) and (b) mixing ratio (g/kg) from AIRS (Amazon-Congo) associated with shallow convection. Percentage of error bars are shown.

3. Results

Figure 2 shows the differences in the average number of aerosol pixels from CALIPSO VFM data sets and mean AIRS water vapor MR associated with shallow (stratocumulus and stratus) clouds between the Amazon and Congo regions. First, we have estimated the total number of the aerosol pixels that surround shallow clouds within a radial distance of 2° from the location of the clouds detected by CloudSat data. We do so in order to avoid the effect of humidification, precipitation scavenging, and false discrimination of aerosols pixels near cloud boundaries in CALIPSO data. Similarly, we compute the MR at each level from the AIRS data. Then we have computed mean values and standard errors of aerosol pixels and water vapor MR surrounding the shallow clouds at each vertical level over each the regions. Figure 2 provides the differences in mean aerosol pixels and MR associated with the shallow clouds in the afternoon at various altitudes. Figure 2a shows that shallow clouds over the Congo region are associated with a higher number of aerosol pixels up to an altitude of 8 km than the Amazon region. On the other hand, shallow clouds over the Amazon region are associated with higher MR throughout the column compared to shallow clouds over the Congo region. Below 700 hPa, an altitude below which shallow clouds generally occur, Amazonian shallow clouds have MR up to 1.4 g/kg higher than the Congo shallow clouds. Such differences in MR between the Amazon and Congo attain a second peak (0.4 g/kg) in the middle troposphere (700–300 hPa) above shallow clouds. A moist free-troposphere ($RH_{700\text{-}300}$) associated with shallow clouds over the Amazon has been noted in the literature and is believed to be related to wet season onset (Wright et al., 2017) and shallow-to-deep convective evolution (Chakraborty, Schiro, et al., 2018). Congo, on the other hand, is a dryer rainforest (Figure 2b) and has higher aerosol concentration compared to the Amazon region (Figure 2a).

In order to understand how afternoon shallow clouds influence the evening deep convection, we show contours of $CTH_{evening}$ as a function of AOD and $CTH_{afternoon}$ in Figure 3 for those clouds that evolve as deep convection in the evening. We do not include clouds that remain shallow (discussed later) in the evening in Figure 3. $CTH_{afternoon}$ is calculated from the CloudSat data and $CTH_{evening}$ is the storm top height detected from the GPM data. Figure 3 shows that $CTH_{evening}$ increases as AOD increases up to 0.7 over the Congo region (Figure 3a). However, $CTH_{evening}$ decreases with $CTH_{afternoon}$ there. A higher $CTH_{afternoon}$ (>4 km) is associated with low-to-moderate $CTH_{evening}$ (~10–12 km), whereas deep convection originating from shallow clouds with $CTH_{afternoon}$ below 4 km can reach a higher altitude ($CTH_{evening}$ > 12 km). Similarly, a decreasing $RR_{evening}$ is associated with an increasing $CTH_{afternoon}$ (Figure 3b). However, such relationships are not observed over the Amazon region (Figures 3c and 3d). Instead, shallow clouds with higher $CTH_{afternoon}$ tend to form deep convection with high $CTH_{evening}$ and a stronger $RR_{evening}$. We also observe similar relationships when we plot contours of $CTH_{evening}$ as a function of $CTH_{afternoon}$ and AIRS CWV (discussed later, Figure 11).

It is apparent that the afternoon shallow clouds have different association with the deep convective development in the evening over the Congo and Amazon regions. We hypothesize that a stronger rainfall in the afternoon could deplete moisture in the troposphere, cool down the ground and the surrounding atmosphere due to the evaporation of hydrometeors, and increase the stability of the atmosphere. Figure 4 shows the mean and standard errors of $RR_{afternoon}$ from GPM IMERG for the afternoon shallow clouds at 1,330, 1,400, and 1,430 pm within a distance of ±0.1° from the location of afternoon shallow clouds detected

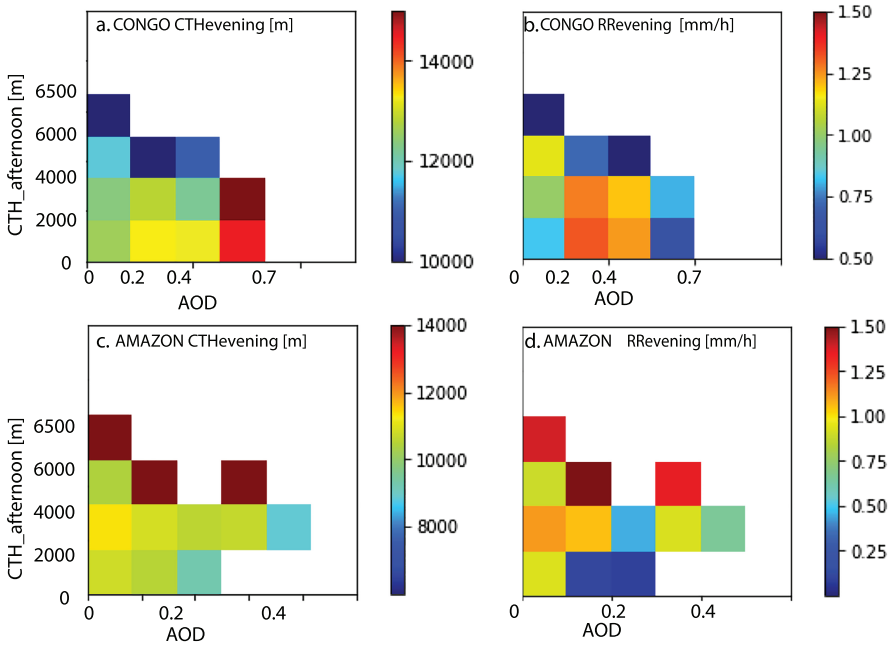

Figure 3. Contours of $CTH_{evening}$ in meters (a, c) and $RR_{evening}$ in millimeter per hour (b, d) over the Congo (a, b) and Amazon (c, d) regions from GPM 2BCMB data as a function of CloudSat Cloud top height in meters (*Y* axis) and TERRA AOD (*X* axis) for clouds that evolve as deep convection in the evening.

from the CloudSat data. Since GPM IMERG data provides rainfall estimates every 30 min, we have computed the mean rainfall between 1,330 and 1,430 pm under each shallow cloud. Location of a shallow cloud is detected from the CloudSat data. The maximum height of a shallow cloud is denoted as their cloud top height and the respective latitude and longitude are taken as the cloud's location. To be consistent with Figure 3, we only compute shallow convective rainfall for those clouds that evolve as deep convection in the evening. Figure 4a shows that $RR_{afternoon}$ increases significantly as shallow cloud's top height increases over the Congo region. Shallow clouds over the Congo region with $CTH_{afternoon}$ less than 2 km have a mean $RR_{afternoon}$ of 0.19 mm/hr. As $CTH_{afternoon}$ increases, mean $RR_{afternoon}$ increases to 0.5, 0.6, 0.9, and 1.1 mm/hr for shallow clouds with $CTH_{afternoon}$ <3, <4, >3, and >4 km, respectively. A stronger rainfall depletes the moisture content of the atmosphere and reduces CAPE. Thus, we compute CAPE and $RH_{700\text{-}300}$ from MERRA2 reanalysis for those cases where shallow convection evolve to deep convection in the evening. We use temperature and specific humidity data set at various pressure levels to compute CAPE, whereas $RH_{700\text{-}300}$ is the free tropospheric humidity or a mean RH between 700 and 300 hPa. Figures 5a and 5b confirm that as $CTH_{afternoon}$ increases, CAPE, and $RH_{700\text{-}300}$ in the evening time (1500 UTC or local time 4 p.m.) decreases, especially as $CTH_{afternoon}$ reaches above 4 km.

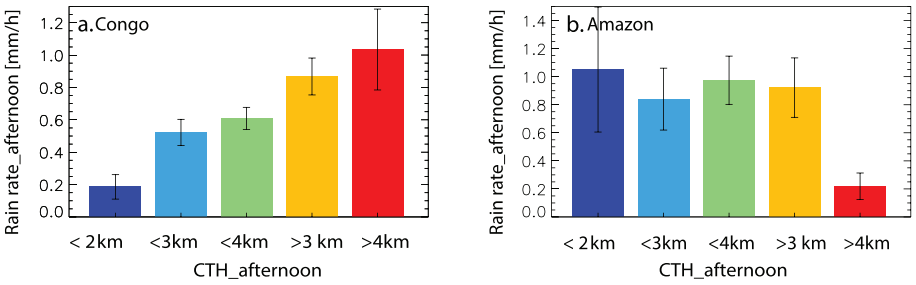

Figure 4. Mean and standard errors of GPM IMERG shallow convective rain rate ($RR_{afternoon}$, mm/hr) at 1,330, 1,400, and 1,430 pm over (a) Congo and (b) Amazon within ±0.1° from the location of CloudSat stratocumulus and stratus clouds for clouds that evolve as deep convection in the evening.

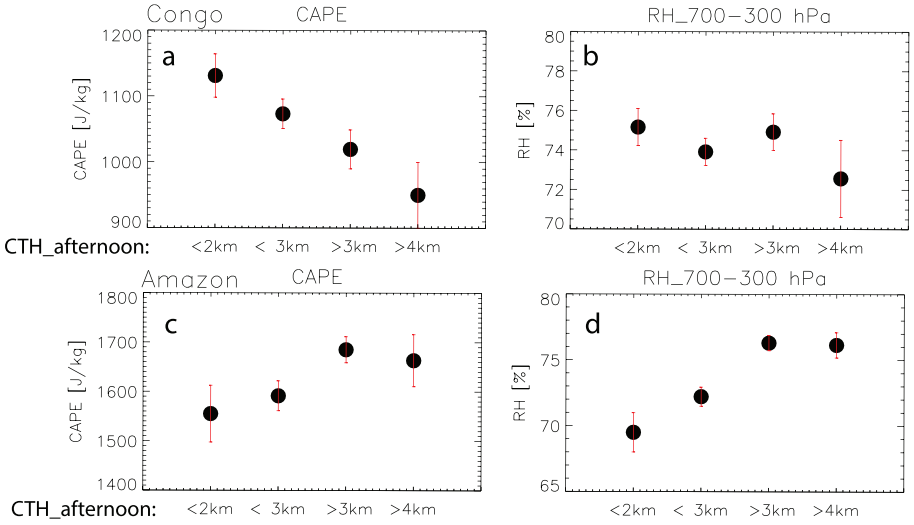

Figure 5. Mean and standard errors of MERRA2 CAPE (a, c), and $RH_{700\text{-}300}$ (b, d) over the Congo (a, b) and Amazon (c, d) regions at 3 p.m. local time for $CTH_{afternoon} < 2$ km, $CTH_{afternoon} < 3$ km, and $CTH_{afternoon} > 3$ km for clouds that evolve as deep convection in the evening.

On the contrary, shallow convective $RR_{afternoon}$ shows no significant increase as their $CTH_{afternoon}$ increases (Figure 4b) over the Amazon region. Evening time CAPE (Figure 5c) and $RH_{700\text{-}300}$ (Figure 5d) also increase with $CTH_{afternoon}$. CAPE associated with deep convection systems that develop from shallow clouds with $CTH_{afternoon}$ >3 km is higher over the Amazon region (~1,500–1,700 J/kg; Figure 5c) than the Congo region (~900–1,150 J/kg; Figure 5a). These results suggest that moisture availability in the free troposphere and CAPE play an important role in the afternoon shallow to the evening deep convection evolutions and also contribute to the differences in such evolutions over these two rainforests.

Deep convection that penetrates to a moderately deep altitude and rains less should also have a reduced amount of LH of condensation released as $CTH_{afternoon}$ increases. In order to verify that, we analyze LH profiles of deep convection using GPM data sets and regress LH released at each level to $CTH_{afternoon}$. Figure 6 shows the rate of change of LH released due to condensation occurring inside the deep convection systems in the evening with $CTH_{afternoon}$ ($\frac{\partial LH}{\partial CTH}$). $\frac{\partial LH}{\partial CTH}$ is estimated by regressing $CTH_{afternoon}$ with LH at each layer. GPM provides LH estimates at 80 levels from the surface to 20 km altitude (every 250 m). The slope of the regression at each level is plotted as $\frac{\partial LH}{\partial CTH}$ against the altitudes in Figure 6. $\frac{\partial LH}{\partial CTH}$ is positive (i.e., condensation increases with $CTH_{afternoon}$) for deep convection systems that develop from shallow clouds with $CTH_{afternoon}$ less than 3 km. However, $\frac{\partial LH}{\partial CTH}$ is negative for deep convection systems that develop from the afternoon time shallow clouds with $CTH_{afternoon}$ >3 km. Such rates are strongly negative for deep convection systems developed from shallow clouds with $CTH_{afternoon}$ >4 km. Thus, it can be inferred from Figures 5 and 6 that as $CTH_{afternoon}$ increases beyond 3 km, LH released due to condensation of the water droplets decreases within deep convection in the evening, consistent with the reduced CAPE and $RH_{700\text{-}300}$ (Figures 5a and 5b). On the other hand, $\frac{\partial LH}{\partial CTH}$ profile is positive over the Amazon region (red line, Figure 6) and is consistent with increasing CAPE and $RH_{700\text{-}300}$ with $CTH_{afternoon}$ (Figures 5c and 5d). It is apparent that afternoon shallow convective rainfall has contrasting influences on the evening time CAPE and $RH_{700\text{-}300}$ over the Amazon and Congo rainforests. It contributes to the LH, $CTH_{evening}$, and $RR_{evening}$ differences over these two regions.

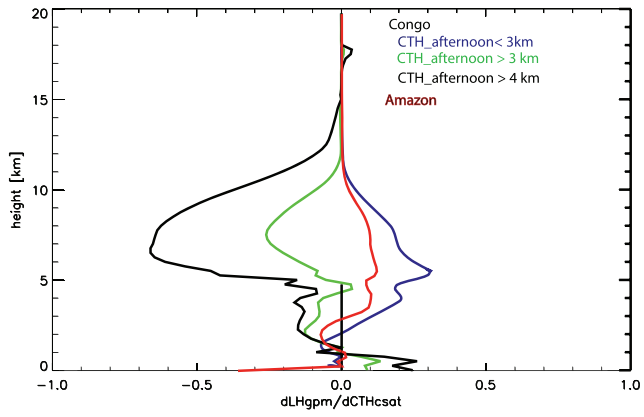

Figure 6. The rate of change of GPM LH from GPM 2HSLH data with CloudSat $CTH_{evening}$ over the Congo region for $CTH_{afternoon}$ <3 km (blue line), $CTH_{afternoon}$ >3 km (green line), $CTH_{afternoon}$ >4 km (black line) and over Amazon (red line) region for clouds that evolve as deep convection in the evening.

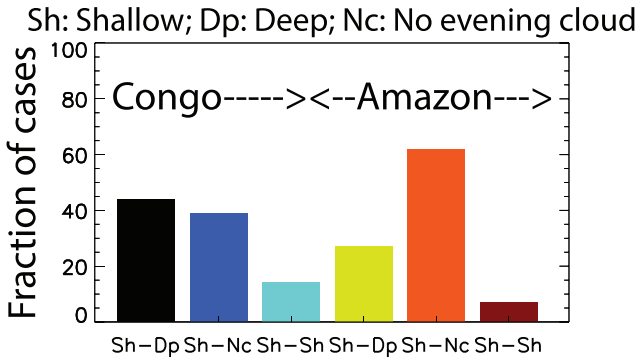

Figure 7. Bar plot of the fraction of convection that evolve as deep (Sh-Dc), remain shallow (Sh-Sh), no cloud (Sh-Nc) in the evening to the total number of shallow clouds in the afternoon over the Congo and Amazon basins.

We have also teased out such relationships for those shallow clouds that remain shallow in the evening. Figure 7 shows the fractions of convection that evolve to deep convection (Sh-Dp), remain shallow (Sh_Sh), or no cloud (no cloud, Sh-Nc) and in the evening. About 45% (30%) shallow clouds over the Congo (Amazon) region evolve to deep convection in the evening. However, about ~15% and ~10% of the afternoon shallow clouds remain shallow over both these regions. Figure 8 shows the $CTH_{evening}$ and $RR_{evening}$ for those clouds that are still shallow (Sh-Sh) as a function of their afternoon cloud top height or $CTH_{afternoon}$ and AOD. Figures 8b and 8d highlight a major difference in between shallow and deep convective $RR_{evening}$. Shallow convective $RR_{evening}$ (Figures 8a and 8c) is significantly less (~0.2 mm/hr) than deep convective $RR_{evening}$ (~1.5 mm/hr; Figures 3b and 3d). Owing to their lower $RR_{evening}$, we turn to analyze their afternoon time rainfall from GPM IMERG data sets (Figure 9). Figure 9 reveals that shallow convective $RR_{afternoon}$ is also less for Sh-Sh clouds, whereas Sh-Dp clouds have a much higher afternoon rain rate in their shallow stages (Figure 4) over both the regions. A comparison of $RR_{evening}$ and $RR_{afternoon}$ between Sh-Sh and Sh-Dp clouds suggests that Sh-Sh in the evening might be associated with lower instability and moisture.

Figure 10 shows the CAPE and $RH_{700\text{-}300}$ associated with the Sh-Sh clouds. The observed difference in CAPE between the Sh-Sh and Sh-Dp (Figure 5) is significant. CAPE associated with Sh-Sh clouds range in between 1,000 and 1,400 (700–900 J/kg) J/kg over the Amazon (Congo) region as compared to 1,500–1,700 (900–1,150) J/kg for Sh-Dp clouds. Sh-Sh clouds are associated with ~5–15% dryer free troposphere than Sh-Dp

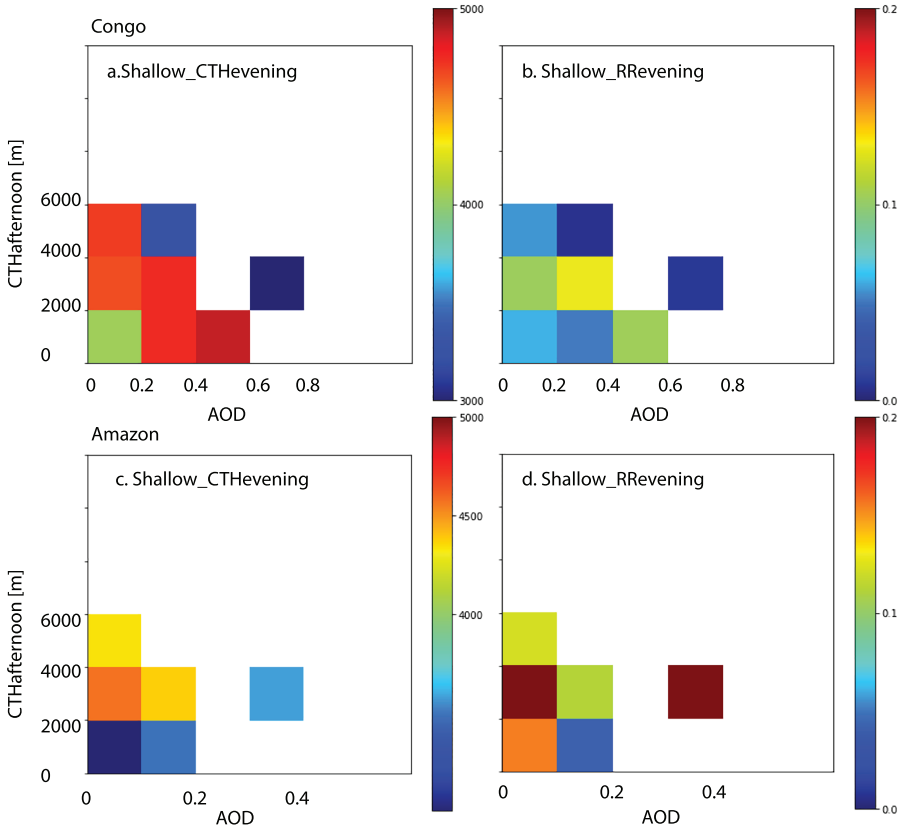

Figure 8. Same as in Figure 3, but for shallow convective top height and rain rate for clouds that remain shallow in the evening.

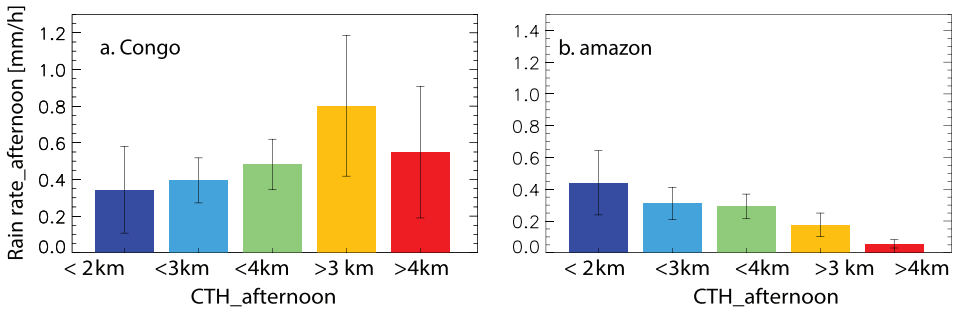

Figure 9. Same as in Figure 4, but for clouds that remain shallow in the evening.

clouds. Thus, CAPE and moisture are the two likely causes for the differences between the Sh-Dp and Sh-Sh clouds.

What happens when we contour $CTH_{evening}$ regardless of whether shallow convection evolve to deeper altitude in the evening are computed as a function of AOD and $CTH_{afternoon}$? Figure 11 shows $CTH_{evening}$ (a and c) over the Congo (a) and Amazon (b) rainforests as a function of shallow convective $CTH_{afternoon}$ from CloudSat and CWV from AIRS data. Here we use CWV to see if the relationship between $CTH_{afternoon}$ and $CTH_{evening}$ observed so far in the analysis is also evident when we use other meteorological parameters such as CWV. Our results show that even after including Sh-Sh clouds, we observe a similar relationship between $CTH_{afternoon}$ and $CTH_{eveving}$ as in Figure 3. $CTH_{evening}$ tends to decrease (increase) as $CTH_{afternoon}$ increases over the Congo (Amazon) region. A higher CWV is associated with deeper clouds in the evening over both the regions and is expected. Associated CAPE and $RH_{700\text{-}300}$ for all the cases show that as $CTH_{afternoon}$ increases over the Congo basin, CAPE and $RH_{700\text{-}300}$ in the evening time (1500 UTC or local time 4 p.m.) decreases, especially as $CTH_{afternoon}$ reaches above 4 km (Figures 11c and 11e). Over the Amazon region, the evening time CAPE (Figure 11d) and $RH_{700\text{-}300}$ (Figure 11f) also increase with $CTH_{afternoon}$. CAPE associated with deep convection systems that develop from shallow clouds with $CTH_{afternoon}$ >3 km is higher over the Amazon region (~1,500–1,600 J/kg; Figure 11d) than the Congo region (~850–950 J/kg; Figure 11c).

Our analyses show $RH_{700\text{-}300}$ and CAPE are two major determinants of the shallow-deep convective mechanism. However, VWS can also play an important role on such evolutions (Chakraborty et al., 2016;

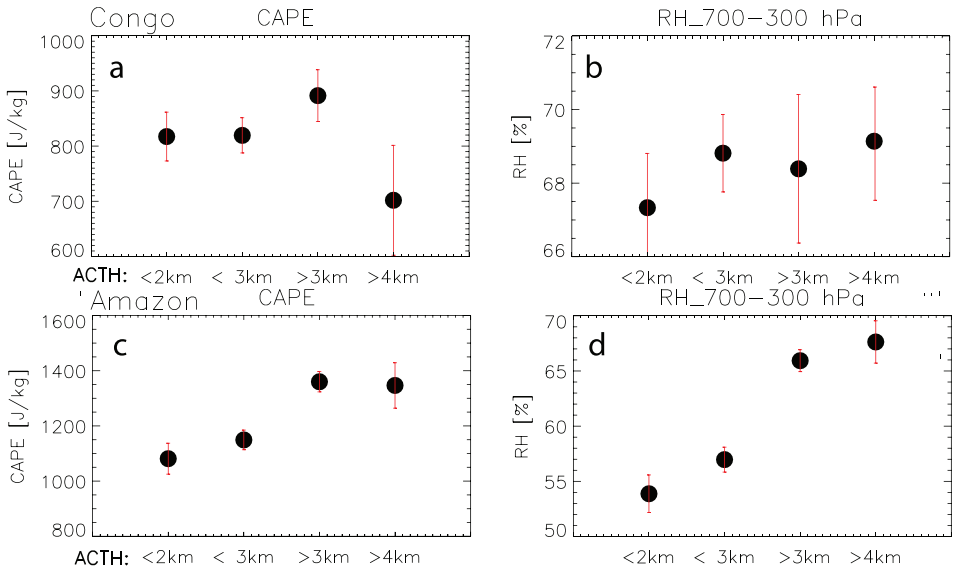

Figure 10. Same as in Figure 5, but for clouds that remain shallow in the evening.

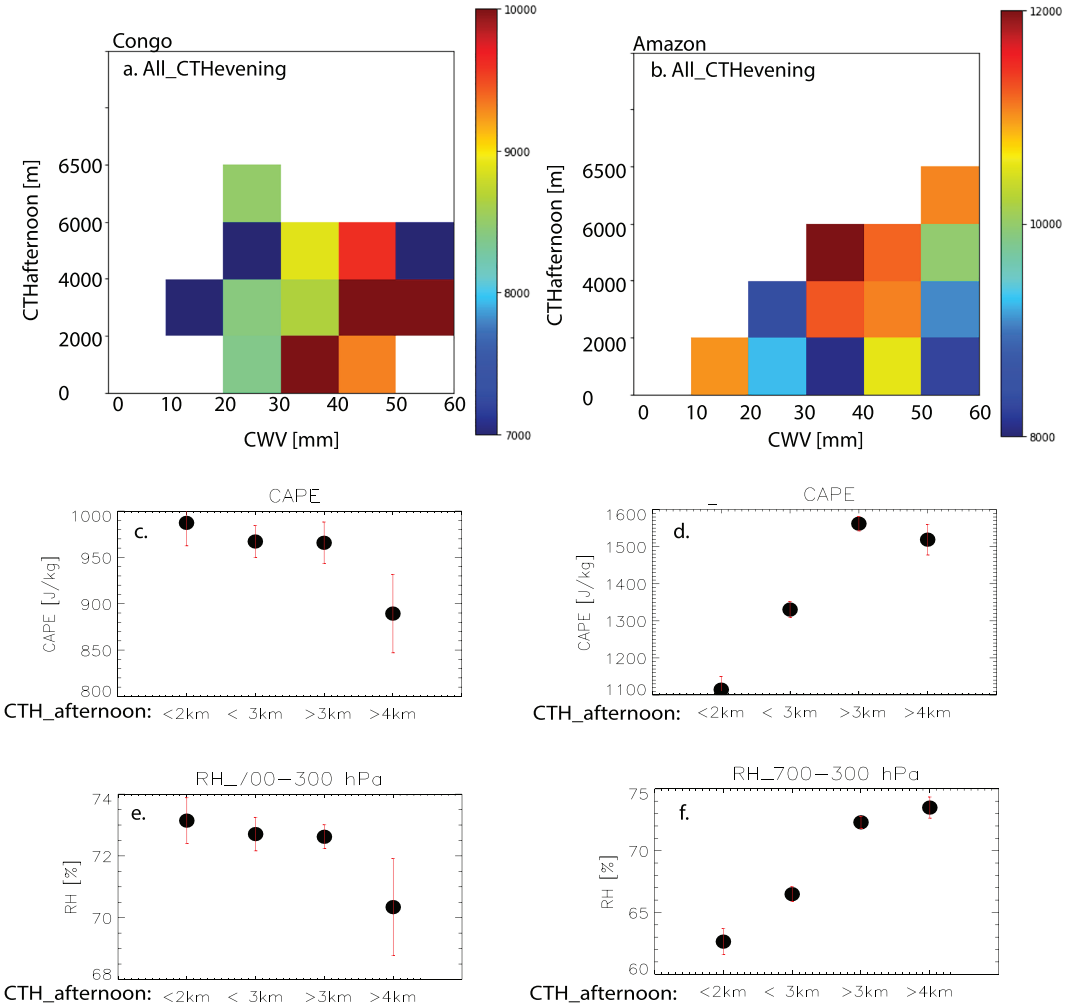

Figure 11. Contours of $CTH_{evening}$ in meters (a, b) over the Congo (a) and Amazon (b) regions from GPM 2BCMB data as a function of CloudSat Cloud top height in meters (*Y* axis) and AIRS CWV (*X* axis) using all the clouds that evolve to deep convection (Sh-Dp) or remain shallow in the evening (Sh-Sh). (c) CAPE associated with all the clouds in (a) over the Congo rainforest, (d) CAPE associated with all the clouds in (b) over the Amazon rainforest, (e) $RH_{700\text{-}300}$ associated with all the clouds in (a) over the Congo rainforest, and (f) $RH_{700\text{-}300}$ associated with all the clouds in (a) over the Congo rainforest. CAPE and $RH_{700\text{-}300}$ are calculated from MERRA2 data sets.

Weisman & Rotunno, 2000, 2004). We show the role of CAPE, $RH_{700\text{-}300}$, VWS, and aerosols on $CTH_{evening}$ for all the clouds regardless of whether those clouds evolve to deep convection in the evening or not. Figures 12a and 12c show that as CAPE and $RH_{700\text{-}300}$ increase, $CTH_{evening}$ increases. Under high CAPE (>1,200 J/kg) and $RH_{700\text{-}300}$ (>60%), evening time cloud top height can reach above 11 km; however, $CTH_{evening}$ limits to below 5 km (or remain shallow) when CAPE is low (<1,200 J/kg) and free troposphere is dry (<40%). VWS (Figures 12b and 12d) play an important role on $CTH_{evening}$. As VWS increases, $CTH_{evening}$ decreases over both the region, presumably because a high wind shear is detrimental for deep convective organization. High VWS tilts and separates the updraft and downdraft regions of the convection in such a way that further development is not possible (Weisman & Rotunno, 2000). Moreover, a stronger wind shear can also influence the thermodynamic properties of the parcel (Chakraborty, Schiro, et al., 2018). Aerosols show a nonlinear relationship with $CTH_{evening}$ over the Congo. As AOD increases, $CTH_{evening}$ increases and then decreases due to condensation loading effect and aerosols' radiative effect (Chakraborty, Fu, et al., 2018; Rosenfeld et al., 2008). Such a non-linear relationship is not observed over the Amazon, presumably because of the fact that convection over the Amazon region are associated with less aerosols.

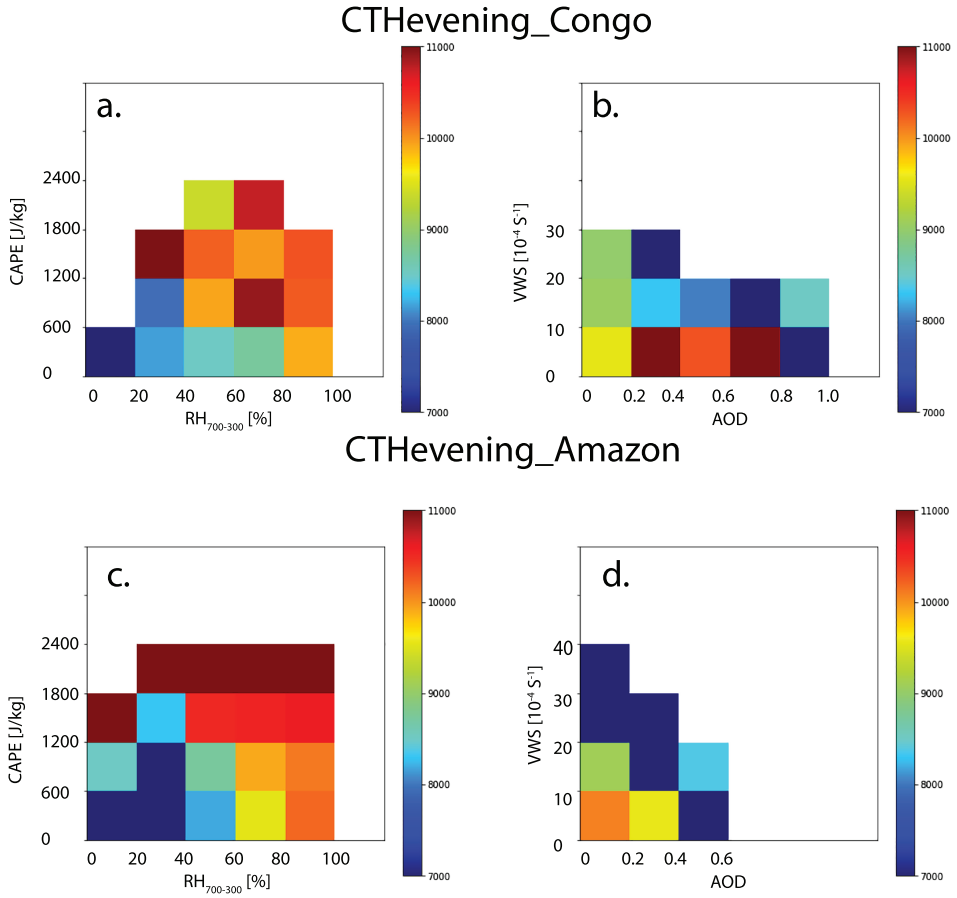

Figure 12. Contours of $CTH_{evening}$ in meters over the Congo (a, b) and Amazon (c, d) regions from GPM 2BCMB data as a function of (a, c) CAPE and $RH_{700\text{-}300}$, (b, d) VWS and AOD using all the clouds that evolve to deep convection (Sh-Dp) or remain shallow in the evening (Sh-Sh).

4. Conclusions and Discussions

Amazon and Congo are the two largest rainforests that are vulnerable to droughts, deforestation, and climate change. Rainfall is tremendously important for the sustainability of these rainforests. Thus, it is important to understand the mechanism behind the evolution of afternoon shallow convection to evening deep convection over the two regions. This study employs information from various satellite data sets to identify the relationship between afternoon shallow clouds and evening deep convection systems over the Congo and Amazon regions.

This study, to our knowledge, is the first that shows the salient differences in the association of the afternoon shallow clouds with the evening deep convective development over the Congo and Amazon regions. Our results suggest that deeper afternoon shallow clouds over the Congo region are linked to suppressed evening deep convection with weakened the evening storm top height and rain rate. As $CTH_{afternoon}$ increases, $CTH_{evening}$ and $RR_{evening}$ decrease over there. On the contrary, shallow clouds over the Amazon region are associated with deeper evening time deep convective cloud. Significant increases in $RH_{700\text{-}300}$ and CAPE in the evening with $CTH_{afternoon}$ over the Amazon occur. This is consistent with an earlier study by Wright et al. (2017), which shows that precipitating shallow clouds increase the relative humidity and column water vapor in the free troposphere, reduce the convective inhibition, increase CAPE, thus destabilize the free troposphere. Such differences are linked to the different environmental conditions over these two regions.

Free tropospheric humidity is one of the key factors in enhancing the buoyancy required for shallow to deep convection evolution over the Amazon region (Chakraborty, Schiro, et al., 2018).

Such a free tropospheric humidification with $CTH_{afternoon}$ does not occur over the Congo shallow clouds. A drier environment as compared to the Amazon region surrounds shallow clouds there. Dry air often intrudes from the Saharan region above 850 hPa (Dezfuli & Nicholson, 2013). As afternoon $RR_{afternoon}$ increases with $CTH_{afternoon}$, moisture is depleted in the free troposphere, CAPE or the buoyancy of the parcel decreases. A reduced CAPE (increased stability) and a drier free troposphere limit the growth of deep convection below 12 km in the evening over the Congo region.

On the other hand, shallow clouds that remain shallow in the evening are also analyzed. Those clouds have less $RR_{afternoon}$ and are associated with weaker CAPE and $RH_{700\text{-}300}$ as compared to Sh-Dc clouds in the evening. They also have less $RR_{evening}$ that is significantly lower (~0.2 mm/hr) than Sh-Dc clouds (~1.5 mm/hr). Thus, it can be concluded from the study that shallow clouds associated with less moisture and instability do not grow deep in the evening and precipitate less during the afternoon as well as in the evening. Such shallow convective behavior is common over both the rainforests. However, shallow clouds that penetrate deep in the evening differ over the Amazon and Congo rainforests. Thus, these differences in the large-scale environmental conditions drive the afternoon shallow to evening deep convective association differently over these two regions.

Along with CAPE and $RH_{700\text{-}300}$ that are favorable for a higher $CTH_{evening}$ (Figures 12a and 12c), we have also analyzed the role of VWS and AOD. As expected, higher VWS are detrimental to deep convective growth as it can tilt the convection and separate the updraft and downdraft region in such a way that further development is not possible. AOD shows a nonlinear relationship (Chakraborty, Fu, et al., 2018; Rosenfeld et al., 2008) with deep convective $CTH_{evening}$ over the Congo basin, but not over the Amazon, presumably due to their association with lower aerosol concentration. Thus, we see the condensate loading and radiation effects on deep convective top height over the Congo basin, but not over the Amazon basin.

This study assumes that deep convection in the evening are spawned from shallow clouds. However, deep convection can propagate from somewhere else. Since convective tracking data are not available during this period, we limit our analysis by dividing the domain in $2° \times 2°$ grid boxes. As mentioned before, we have carried out the search for shallow clouds in each grid and if we detect the presence of any deep cloud within that grid, we discard that grid from our analysis. We could not perform a separate analysis based on the seasonality (dry or wet) due to the limitation of samples. In future, with the availability of more data from GPM, we can revisit to see if the relationships differ between seasons. We have used GPM data sets to detect the storm top height in the evening. GPM is 35-GHz radar and can detect particles larger than Cloudsat, which is 94-GHz radar. This mismatch between CloudSat and GPM is a limitation of this study. As a result, a storm with top height above 8 km detected by GPM radar is chosen as a deep convection. This study uses stratus and stratocumulus as shallow clouds. It can be expanded in the future to see the influence from cumulus clouds, which are low to moderately thick clouds according to CloudSat cloud Classification.

Acknowledgments
This study was supported by the NASA ROSES ACMAP and CCST funding. The research was carried out at Jet Propulsion Laboratory, California Institute of Technology, under a contract with the National Aeronautics and Space Administration. R. F. conducted the work at University of California, Los Angeles. The satellite data used in this study can be downloaded from the NASA Earth data Distribution Active Archive Centers (DAACs; at https://earthdata.nasa.gov/about/daacs). MERRA-2 data can be downloaded online (https://gmao.gsfc.nasa.gov/reanalysis/MERRA-2/data_access/).

References

Aragao, L. E. O. C., Anderson, L. O., Fonseca, M. G., Rosan, T. M., Vedovato, L. B., Wagner, F. H., et al. (2018). 21st century drought-related fires counteract the decline of Amazon deforestation carbon emissions. *Nature Communications*, *9*(1), 536. https://doi.org/10.1038/s41467-017-02771-y

Chakraborty, S., Fu, R., Massie, S. T., & Stephens, G. (2016). Relative influence of meteorological conditions and aerosols on the lifetime of mesoscale convective systems. *Proceedings of the National Academy of Sciences of the United States of America*, *113*(27), 7426–7431.

Chakraborty, S., Fu, R., Rosenfeld, D., & Massie, S. T. (2018). The influence of aerosols and meteorological conditions on the total rain volume of the mesoscale convective systems over tropical continents. *Geophysical Research Letters*, *45*, 13099–13106. https://doi.org/10.1029/2018GL080371

Chakraborty, S., Fu, R., Wright, J. S., & Massie, S. T. (2015). Relationships between convective structure and transport of aerosols to the upper troposphere deduced from satellite observations. *Journal of Geophysical Research: Atmospheres*, *120*, 6515–6536. https://doi.org/10.1002/2015JD023528

Chakraborty, S., Schiro, K. A., Fu, R., & Neelin, J. D. (2018). On the role of aerosols, humidity, and vertical wind shear in the transition of shallow to deep convection at the Green Ocean Amazon 2014/5 site. *Atmospheric Chemistry and Physics Discussions*, *36*.

Chu, D. A., Kaufman, Y. J., Ichoku, C., Remer, L. A., Tanre, D., & Holben, B. N. (2002). Validation of MODIS aerosol optical depth retrieval over land. *Geophysical Research Letters*, *29*(12), 8007. https://doi.org/10.1029/2001GL013205

Cook, K. H., & Vizy, E. K. (2016). The Congo Basin Walker circulation: Dynamics and connections to precipitation. *Climate Dynamics*, *47*(3-4), 697–717.

Cox, P. M., Betts, R. A., Collins, M., Harris, P. P., Huntingford, C., & Jones, C. D. (2004). Amazonian forest dieback under climate-carbon cycle projections for the 21st century. *Theoretical and Applied Climatology*, *78*(1-3), 137–156.

Del Genio, A. D., & Wu, J. B. (2010). The role of entrainment in the diurnal cycle of continental convection. *Journal of Climate*, *23*(10), 2722–2738.

Dezfuli, A. K., & Nicholson, S. E. (2013). The relationship of rainfall variability in Western Equatorial Africa to the tropical oceans and atmospheric circulation. Part II: The boreal autumn. *Journal of Climate*, *26*(1), 66–84.
Feng, S., & Fu, Q. (2013). Expansion of global drylands under a warming climate. *Atmospheric Chemistry and Physics*, *13*(19), 10081–10094.
Fu, R., Dickinson, R. E., Chen, M. X., & Wang, H. (2001). How do tropical sea surface temperatures influence the seasonal distribution of precipitation in the equatorial Amazon? *Journal of Climate*, *14*(20), 4003–4026.
Fu, R., Zhu, B., & Dickinson, R. E. (1999). How do atmosphere and land surface influence seasonal changes of convection in the tropical Amazon? *Journal of Climate*, *12*(5), 1306–1321.
Gelaro, R., McCarty, W., Suárez, M. J., Todling, R., Molod, A., Takacs, L., et al. (2017). The Modern-Era Retrospective Analysis for Research and Applications, Version 2 (MERRA-2). *Journal of Climate*, *30*(14), 5419–5454. https://doi.org/10.1175/JCLI-D-16-0758.1
Hagan, D. E., Webster, C. R., Farmer, C. B., May, R. D., Herman, R. L., Weinstock, E. M., et al. (2004). Validating AIRS upper atmosphere water vapor retrievals using aircraft and balloon in situ measurements. *Geophysical Research Letters*, *31*, L21103. https://doi.org/10.1029/2004GL020302
Houze, R. A. (2004). Mesoscale convective systems. *Reviews of Geophysics*, *42*, RG4003. https://doi.org/10.1029/2004RG000150
Hua, W. J., Zhou, L. M., Nicholson, S. E., Chen, H. S., & Qin, M. H. (2019). Assessing reanalysis data for understanding rainfall climatology and variability over Central Equatorial Africa. *Climate Dynamics*, *53*(1-2), 651–669.
Huffman, G. J., Bolvin, D. T., Braithwaite, D., Hsu, K., Joyce, R., & Xie, P. (2014). NASA Global Precipitation Measurement Integrated Multi-satellitE Retrievals for GPM (IMERG). , *Algorithm Theoretical Basis Doc., version 4.4, 30 pp*.
Jensen, M. P., & Del Genio, A. D. (2006). Factors limiting convective cloud-top height at the ARM Nauru Island climate research facility. *Journal of Climate*, *19*(10), 2105–2117.
Jones, T. A., & Stensrud, D. J. (2012). Assimilating AIRS temperature and mixing ratio profiles using an ensemble Kalman filter approach for convective-scale forecasts. *Weather and Forecasting*, *27*(3), 541–564.
Laurance, W. F., Fearnside, P. M., Laurance, S. G., Delamonica, P., Lovejoy, T. E., Rankin-de Merona, J., et al. (1999). Relationship between soils and Amazon forest biomass: A landscape-scale study. *Forest Ecology and Management*, *118*(1-3), 127–138.
Li, W. H., Fu, R., & Dickinson, R. E. (2006). Rainfall and its seasonality over the Amazon in the 21st century as assessed by the coupled models for the IPCC AR4. *Journal of Geophysical Research*, *111*, D02111. https://doi.org/10.1029/2005JD006355
Liu, J. J., Chen, B., & Huang, J. P. (2014). Discrimination and validation of clouds and dust aerosol layers over the Sahara desert with combined CALIOP and IIR measurements. *Journal of Meteorological Research*, *28*(2), 185–198.
Liu, Z. Y., Vaughan, M., Winker, D., Kittaka, C., Getzewich, B., Kuehn, R., et al. (2009). The CALIPSO lidar cloud and aerosol discrimination: Version 2 algorithm and initial assessment of performance. *Journal of Atmospheric and Oceanic Technology*, *26*(7), 1198–1213.
Malhi, Y., & Wright, J. (2004). Spatial patterns and recent trends in the climate of tropical rainforest regions. *Philosophical Transactions of the Royal Society B*, *359*(1443), 311–329.
Molion, L. C. B. (1975). A climatonomic study of the energy and moisture fluxes of the Amazonas Basin with considerations of deforestation effects, Thesis (PH.D.)--THE UNIVERSITY OF WISCONSIN - MADISON thesis.
Neupane, N. (2016). The Congo basin zonal overturning circulation. *Advances in Atmospheric Sciences*, *33*(6), 767–782.
Nicholson, S. E. (2017). Climate and climatic variability of rainfall over eastern Africa. *Reviews of Geophysics*, *55*, 590–635. https://doi.org/10.1002/2016RG000544
Nicholson, S. E., & Dezfuli, A. K. (2013). The relationship of rainfall variability in western equatorial Africa to the tropical oceans and atmospheric circulation. Part I: The boreal spring. *Journal of Climate*, *26*(1), 45–65.
Nicholson, S. E., Klotter, D., Zhou, L., & Hua, W. (2019). Validation of satellite precipitation estimates over the Congo Basin. *Journal of Hydrometeorology*, *20*(4), 631–656.
Petersen, W. A., Fu, R., Chen, M. X., & Blakeslee, R. (2006). Intraseasonal forcing of convection and lightning activity in the southern Amazon as a function of cross-equatorial flow. *Journal of Climate*, *19*(13), 3180–3196.
Phillips, O. L., Aragão, L. E., Lewis, S. L., Fisher, J. B., Lloyd, J., López-González, G., et al. (2009). Drought sensitivity of the Amazon rainforest. *Science*, *323*(5919), 1344–1347. https://doi.org/10.1126/science.1164033
Raghavendra, A., Zhou, L. M., Jiang, Y., & Hua, W. J. (2018). Increasing extent and intensity of thunderstorms observed over the Congo Basin from 1982 to 2016. *Atmospheric Research*, *213*, 17–26.
Redemann, J., Vaughan, M. A., Zhang, Q., Shinozuka, Y., Russell, P. B., Livingston, J. M., et al. (2012). The comparison of MODIS-Aqua (C5) and CALIOP (V2 & V3) aerosol optical depth. *Atmospheric Chemistry and Physics*, *12*(6), 3025–3043.
Remer, L. A., Kaufman, Y. J., Tanré, D., Mattoo, S., Chu, D. A., Martins, J. V., et al. (2005). The MODIS aerosol algorithm, products, and validation. *Journal of the Atmospheric Sciences*, *62*(4), 947–973. https://doi.org/10.1175/JAS3385.1
Remer, L. A., Webster, C. R., Farmer, C. B., May, R. D., Herman, R. L., Weinstock, E. M., et al. (2002). Validation of MODIS aerosol retrieval over ocean. *Geophysical Research Letters*, *29*(12), 8008. https://doi.org/10.1029/2001GL013204
Rienecker, M. M., Suarez, M. J., Gelaro, R., Todling, R., Bacmeister, J., Liu, E., et al. (2011). MERRA: NASA's Modern-Era Retrospective Analysis for Research and Applications. *Journal of Climate*, *24*(14), 3624–3648. https://doi.org/10.1175/JCLI-D-11-00015.1
Rosenfeld, D., Lohmann, U., Raga, G. B., O'Dowd, C. D., Kulmala, M., Fuzzi, S., et al. (2008). Flood or drought: How do aerosols affect precipitation? *Science*, *321*(5894), 1309–1313. https://doi.org/10.1126/science.1160606
Salati, E., & Vose, P. B. (1984). Amazon Basin—A system in equilibrium. *Science*, *225*(4658), 129–138. https://doi.org/10.1126/science.225.4658.129
Sassen, K., & Wang, Z. (2008). Classifying clouds around the globe with the CloudSat radar: 1-year of results. *Geophysical Research Letters*, *35*, L04805. https://doi.org/10.1029/2007GL032591
Sungmin, O., Foelsche, U., Kirchengast, G., Fuchsberger, J., Tan, J., & Petersen, W. A. (2017). Evaluation of GPM IMERG Early, Late, and Final rainfall estimates using WegenerNet gauge data in southeastern Austria. *Hydrology and Earth System Sciences*, *21*(12), 6559–6572.
Tackett, J. L., & Di Girolamo, L. (2009). Enhanced aerosol backscatter adjacent to tropical trade wind clouds revealed by satellite-based lidar. *Geophysical Research Letters*, *36*, L14804. https://doi.org/10.1029/2009GL039264
Tyukavina, A., Hansen, M. C., Potapov, P., Parker, D., Okpa, C., Stehman, S. V., et al. (2018). Congo Basin forest loss dominated by increasing smallholder clearing. *Science Advances*, *4*(11), eaat2993. https://doi.org/10.1126/sciadv.aat2993
Varnai, T., & Marshak, A. (2009). MODIS observations of enhanced clear sky reflectance near clouds. *Geophysical Research Letters*, *36*, L06807. https://doi.org/10.1029/2008GL037089
Vera, C., Silvestri, G., Liebmann, B., & Gonzalez, P. (2006). Climate change scenarios for seasonal precipitation in South America from IPCC-AR4 models. *Geophysical Research Letters*, *33*, L13707. https://doi.org/10.1029/2006GL025759
Wang, Z., & Sassen, K. (2001). Cloud type and macrophysical property retrieval using multiple remote sensors. *Journal of Applied Meteorology*, *40*(10), 1665–1682.

Washington, R., James, R., Pearce, H., Pokam, W. M., & Moufouma-Okia, W. (2013). Congo Basin rainfall climatology: Can we believe the climate models? *Philosophical Transactions of the Royal Society B*, *368*(1625). https://doi.org/10.1098/rstb.2012.0296

Weisman, M. L., & Rotunno, R. (2000). The use of vertical wind shear versus helicity in interpreting supercell dynamics. *Journal of the Atmospheric Sciences*, *57*(9), 1452–1472.

Weisman, M. L., & Rotunno, R. (2004). "A theory for strong long-lived squall lines" revisited. *Journal of the Atmospheric Sciences*, *61*(4), 361–382.

Whittleston, D., Nicholson, S. E., Schlosser, A., & Entekhabi, D. (2017). Climate models lack jet-rainfall coupling over West Africa. *Journal of Climate*, *30*(12), 4625–4632.

Wright, J. S., Fu, R., Worden, J. R., Chakraborty, S., Clinton, N. E., Risi, C., et al. (2017). Rainforest-initiated wet season onset over the southern Amazon. *Proceedings of the National Academy of Sciences*, *114*(32), 8481–8486. https://doi.org/10.1073/pnas.1621516114

Zhou, L. M., Tian, Y., Myneni, R. B., Ciais, P., Saatchi, S., Liu, Y. Y., et al. (2014). Widespread decline of Congo rainforest greenness in the past decade. *Nature*, *509*(7498), 86–90. https://doi.org/10.1038/nature13265

Zhuang, Y. Z., Fu, R., Marengo, J. A., & Wang, H. Q. (2017). Seasonal variation of shallow-to-deep convection transition and its link to the environmental conditions over the Central Amazon. *Journal of Geophysical Research: Atmospheres*, *122*, 2649–2666. https://doi.org/10.1002/2016JD025993